Merifield, R. S., Sloan, S. W. & Yu, H. S. (2001). *Géotechnique* **51**, No. 2, 141–153

Stability of plate anchors in undrained clay

R. S. MERIFIELD,* S. W. SLOAN* AND H. S. YU*

Soil anchors are commonly used as foundation systems for structures requiring uplift resistance, such as transmission towers, or for structures requiring lateral resistance, such as sheet pile walls. To date, the design of these anchors has been largely based on empiricism. This paper applies numerical limit analysis to rigorously evaluate the stability of vertical and horizontal strip anchors in undrained clay. Rigorous bounds on the ultimate pull-out capacity are obtained by using two numerical procedures that are based on finite element formulations of the upper and lower bound theorems of limit analysis. These formulations follow standard procedure by assuming a rigid perfectly plastic clay model with a Tresca yield criterion, and generate large linear programming problems. By obtaining both upper and lower bound estimates of the pull-out capacity, the true pull-out resistance can be bracketed from above and below. Results are presented in the familiar form of break-out factors based on various soil strength profiles and geometries, and are compared with existing numerical and empirical solutions.

KEYWORDS: anchors; clays; failure; numerical modelling; plasticity; suction.

Les ancrages de scellement sont utilisés couramment comme systèmes de fondation pour les structures qui demandent une résistance au relèvement, comme les tours de transmissions, ou pour les structures demandant une résistance latérale, comme les murs de palplanches. A ce jour, la forme de ces ancrages a été le plus souvent déterminée de manière empirique. Cet exposé applique l'analyse de limite numérique pour évaluer de manière rigoureuse la stabilité des bandes d'ancrage verticales et horizontales dans de l'argile non drainée. Nous obtenons des limites rigoureuses de la capacité de retenue ultime en utilisant deux procédures numériques qui sont basées sur les formules d'éléments finis des théorèmes de limite supérieure et inférieure d'analyse limite. Ces formules suivent une procédure standard en supposant un modèle d'argile rigide parfaitement plastique avec un critère d'élasticité Tresca et elles produisent d'importants problèmes de programmation linéaire. En obtenant les estimations de limite supérieure et inférieure de la capacité de retenue, la véritable résistance de retenue peut être cernée par le haut et par le bas. Nous présentons les résultats sous la forme familière de facteurs de décrochement basés sur divers profils et géométries de résistance du sol ; ces résultats sont comparés aux solutions numériques et empiriques existantes.

INTRODUCTION

Background and objectives

The design of many engineering structures requires foundation systems to resist vertical uplift or horizontal pullout forces. These type of structures, which may include transmission towers or earth-retaining walls, are commonly supported directly by soil anchors. More recently, anchors have been used to provide a simple and economical mooring system for offshore floating oil and gas facilities. As the range of applications for anchors expands to include the support of more elaborate and substantially larger structures, a greater understanding of their behaviour is required.

The objectives of the present paper are: (1) to present rigorous bounding solutions for the ultimate capacity of horizontal and vertical strip anchors in both homogeneous and inhomogeneous clay soils; and (2) to compare these limit analysis solutions with empirical and numerical results presented previously in the literature by a number of authors. The effect of anchor plate roughness upon the ultimate capacity will also be considered.

Previous studies

During the last 30 years a number of researchers have proposed approximate techniques to estimate the ultimate uplift capacity of anchors in various soil types. Most existing theoretical and experimental research, however, has focused on predicting anchor behaviour and capacity in sand. In contrast, the study of anchors embedded in undrained clay has attracted only limited attention. A comprehensive overview on the topic of anchors is given by Das (1990).

Most of the results from studies of anchors in clay either consist of simple analytical solutions or are derived empirically from laboratory model tests. These results can be found in the works of Meyerhof & Adams (1968), Vesic (1971), Meyerhof (1973), Das (1978, 1980), Ranjan & Arora (1980), and Das *et al.* (1985a, 1985b). The uplift capacity of anchors is typically expressed in terms of a break-out factor, which is a function of the anchor shape, embedment depth, overburden pressure and the soil properties.

In contrast to the variety of experimental results discussed above, very few numerical analyses have been performed to determine the pull-out capacity of anchors in clay, with the most rigorous study being by Rowe & Davis (1982). In their paper, results were presented for both horizontal and vertical strip anchors embedded in homogeneous saturated clay. These were obtained using an elasto-plastic finite element analysis that incorporated soil–structure interaction theory at the soil/anchor boundary. The effects of anchor roughness, thickness and shape were also considered. Other displacement finite element studies on the behaviour of anchors in clay have been made by Ashbee (1969) and Davie & Sutherland (1977), although very limited results were reported.

Although the limit theorems provide a simple and useful way of analysing the stability of geotechnical structures, they have not been widely applied to the problem of anchors in soil. Numerical upper and lower bound techniques have recently been used to study numerous problems including the undrained stability of a trapdoor (Sloan *et al.*, 1990), the stability of slopes (Yu *et al.*, 1998), the bearing capacity of foundations (Yu & Sloan, 1994; Merifield *et al.*, 1999; Ukritchon *et al.*, 1998), and reinforced soils (Yu & Sloan, 1997), and tunnels Sloan & Assadi, 1991 & 1992.

Rowe (1978) and Gunn (1980) used the bound theorems to produce simple solutions for the case of a horizontal strip

Manuscript received 24 January 2000; revised manuscript accepted 9 October 2000.
Discussion on this paper closes 6 September; for further details see inside front cover.
* Department of Civil, Surveying and Environmental Engineering, University of Newcastle, Australia.

anchor and trapdoor respectively. However, owing to the difficulty in manually constructing statically admissible (lower bound) stress fields and kinematically admissible (upper bound) velocity fields, the simple solutions obtained were unable to bracket the pull-out capacity to sufficient accuracy. The purpose of this paper is to take full advantage of the ability of recent numerical formulations of the limit theorems to bracket the actual collapse load accurately from above and below. The lower and upper bounds are computed, respectively, using the numerical techniques developed by Sloan (1988) and Sloan & Kleeman (1995).

PROBLEM OF ANCHOR CAPACITY

Problem definition

Soil anchors may be positioned either vertically or horizontally depending on the load orientation or type of structure requiring support. Anchors are typically constructed from steel or concrete, and can be circular (including helical), square or rectangular in shape. A general layout of the problem to be analysed is shown in Fig. 1.

After Rowe & Davis (1982), the analysis of anchor behaviour can be divided into two distinct categories, namely those of *immediate breakaway* and *no breakaway.* In the immediate breakaway case it is assumed that the soil/anchor interface cannot sustain tension, so that, upon loading, the vertical stress immediately below the anchor reduces to zero and the anchor is no longer in contact with the underlying soil. This represents the case where there is no adhesion or suction between the soil and anchor. In the no breakaway case the opposite is assumed, with the soil/anchor interface sustaining adequate tension to ensure the anchor remains in contact with the soil at all times. This models the case where an adhesion or suction exists between the anchor and the soil. In reality it is likely that the true breakaway state will fall somewhere between the extremities of the immediate breakaway and no breakaway cases.

The suction force developed between the anchor and soil is likely to be a function of several variables, including the embedment depth, soil permeability, undrained shear strength and loading rate. The actual magnitude of any adhesion or suction force is therefore highly uncertain, and should not be relied upon in the routine design of anchors. For this reason, the anchor analyses presented in this paper are performed for the immediate breakaway case only. This will result in conservative estimates of the actual pull-out resistance with suction.

After allowing for immediate and no breakaway behaviour, anchors can be further classified as shallow or deep, depending on their mode of failure. This point is illustrated in Fig. 2. An anchor is classified as shallow if, at ultimate collapse, the observed failure mechanism reaches the surface (Fig. 2(a), (b)). In contrast, a deep anchor is one whose failure mode is characterized by localized shear around the anchor and is not affected by the location of the soil surface (Fig. 2(c)).

For a given anchor size, B, and soil type, (γ, c_u), there exists a critical embedment depth, H_{cr}, at which the failure mechanism no longer extends to the soil surface and becomes fully localised around the anchor. When this type of behaviour occurs, the ultimate capacity of the anchor will have reached a maximum limiting value. Physically, this transition arises because the undrained shear strength is assumed to be independent of the mean normal stress. From a practical point of view, this result is important as embedding the anchor beyond H_{cr} will not lead to an appreciable increase in anchor capacity, Q_u (see Fig. 2(d)).

In light of the above discussion it is proposed to present the anchor capacity, q_u, in a form similar to that outlined by Rowe (1978), which can account for both inhomogeneous material and deep anchor behaviour.

Pull-out capacity of anchors in undrained clay

For a inhomogeneous soil profile, the change in soil cohesion with depth is assumed to vary linearly according to

$$c_u(z) = c_{uo} + \rho z$$

where c_{uo} is the undrained shear strength at the ground surface, z is the depth below the ground surface, and $\rho = dc_u/dz$.

In this paper, theoretical solutions are derived for problems where H/B ranges from 1 to 10 and $\rho B/c_{uo}$ varies from 0·1 to 1. It is anticipated that this will cover most problems of practical interest.

The ultimate anchor pull-out capacity in undrained clay is usually expressed as a function of the undrained shear strength in the following form:

$$q_u = c_u N_c \tag{1}$$

where for a homogeneous soil profile

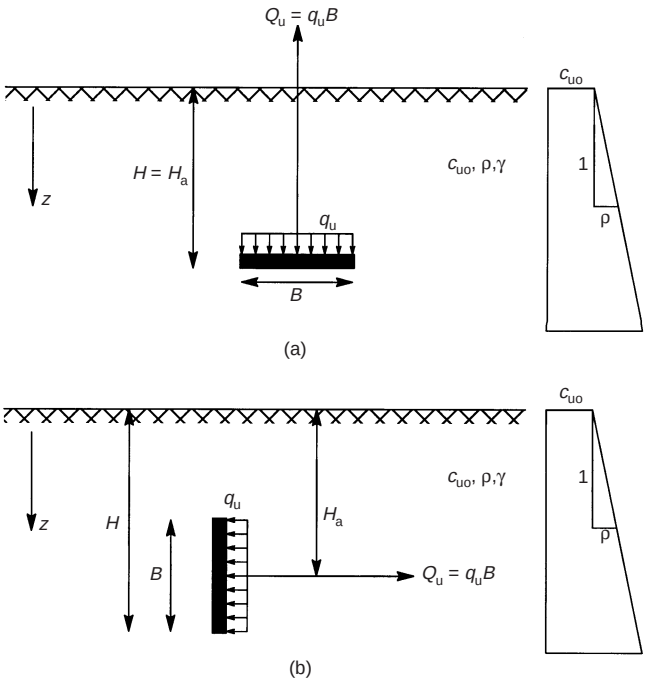

Fig. 1. Problem notation: (a) horizontal plate anchors; (b) vertical plate anchors

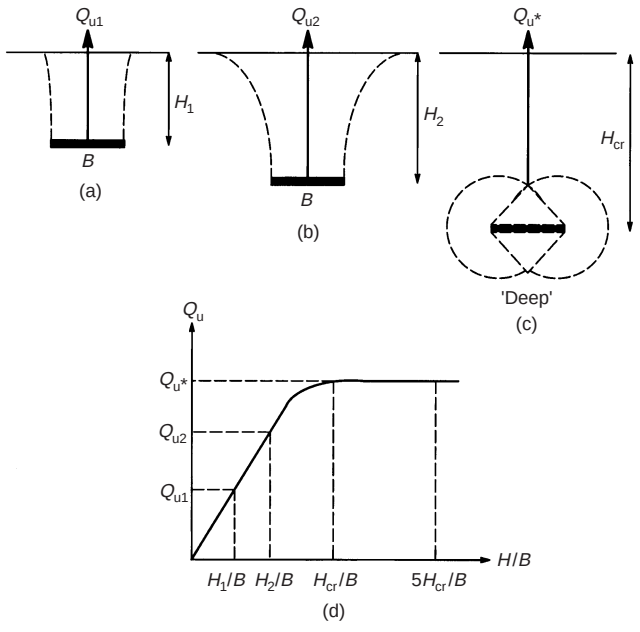

Fig. 2. Shallow and deep anchor behaviour

$$N_c = \left(\frac{q_u}{c_u}\right)_{\gamma\neq 0,\rho=0} = N_{co} + \frac{\gamma H_a}{c_u} \tag{2}$$

and the term N_{co} is defined as

$$N_{co} = \left(\frac{q_u}{c_u}\right)_{\gamma=0,\rho=0} \tag{3}$$

For an inhomogeneous soil profile, the break-out factor can be expressed as

$$N_c = \left(\frac{q_u}{c_{uo}}\right)_{\gamma\neq 0,\rho\neq 0} = N_{co\rho} + \frac{\gamma H_a}{c_{uo}} \tag{4}$$

where $N_{co\rho}$ is defined as

$$N_{co\rho} = \left(\frac{q_u}{c_{uo}}\right)_{\gamma=0,\rho\neq 0} \tag{5}$$

with $H_a = H$ for horizontal anchors and $H_a = H - B/2$ for vertical anchors (see Fig. 2(b)).

Implicit in equation (1) is the assumption that the effects of soil unit weight and cohesion are independent of each other and may be superimposed. It will be shown that this assumption generally provides a good approximation to the behaviour of purely cohesive undrained clay.

The above equations reflect the complex nature of the break-down factor, N_c, as observed by Rowe (1978), which is a function of both the embedment ratio and overburden pressure. The latter dependence is expressed in terms of the dimensionless quantity $\gamma H_a/c_u$ and implies that if the ratio of $\gamma H_a/c_u$ is large enough, then the anchor will behave as a deep anchor even at shallow embedment depths. This will be discussed in a later section of this paper.

FINITE ELEMENT LIMIT ANALYSIS

The following is only a brief summary of the numerical formulation of the limit theorems, and only those aspects specifically related to the current study of anchor capacity are mentioned. Full details of the numerical procedures can be found in Sloan (1988) and Sloan & Kleeman (1995), and will not be repeated here.

Finite element lower bound formulation

The lower bound solution is obtained by modelling a statically admissible stress field using finite elements where stress discontinuities can occur at the interface between adjacent elements. Application of the stress boundary conditions, equilibrium equations and yield criterion leads to an expression for the collapse load that is maximised subject to a set of linear constraints on the stresses.

In the finite element methods, the stress field can be modelled under plane strain conditions using three types of elements. The body of the mesh is comprised of three-noded triangular elements, while along the infinite boundaries triangular and rectangular extension elements are used. The unknown stresses within each element are assumed to vary linearly. Including extension elements in the lower bound mesh permits the stress field to be extended throughout the semi-infinite domain of the problem without violating equilibrium, the stress boundary conditions, or the yield criterion. This ensures that the stress field is truly statically admissible, and that a rigorous lower bound estimate of the collapse load will be found.

Unlike the more familiar displacement finite element method, each node is unique to a particular element and therefore any number of nodes may share the same coordinates. This enables a wide range of stress fields to be modelled by permitting statically admissible stress discontinuities at all edges that are shared by adjacent elements, including those edges that are shared by adjacent extension elements. To furnish a rigorous lower bound solution for the collapse load it is necessary to ensure that the stress field obeys equilibrium, the stress boundary conditions and the yield criterion. Each of these requirements imposes a separate set of constraints on the nodal stresses. The present analyses assume that the undrained shear strength of the clay can be represented by the Tresca yield criterion, which is replaced by a series of linear inequalities (Sloan, 1988). This linear approximation, which is known as a linearised yield surface, is defined to be internal to the Tresca yield surface to preserve the lower bound property of the solution.

A typical lower bound mesh for a vertical anchor, along with the applied stress boundary conditions, is shown in Fig. 3. To model a perfectly rough anchor, no constraints are placed on the shear stress developed at element nodes located directly in front of and behind the anchor. The shear stress is therefore unrestricted, and may vary up to a value less than or equal to the undrained shear strength of the soil (according to the yield constraint). Alternatively, a smooth anchor is modelled by insisting that the shear stress is zero at all element nodes along the anchor/soil interface. To allow the rear side of the anchor to separate from the soil (immediate breakaway), the stress discontinuity behind the anchor is removed and the shear stress and normal stress are forced to be equal to zero. This effectively creates a free surface behind the anchor.

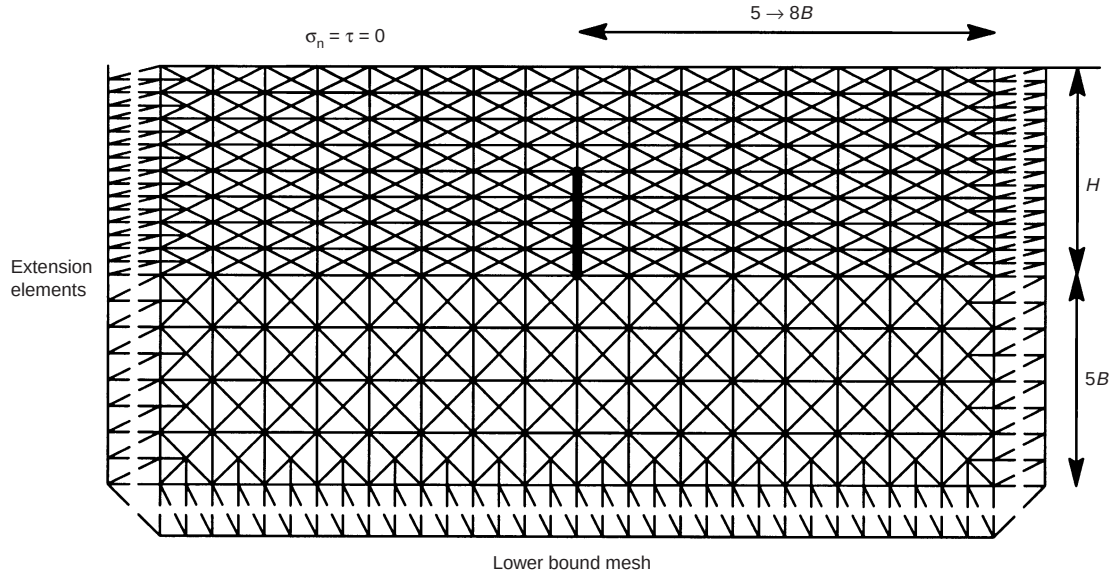

Fig. 3. Typical finite element mesh for vertical anchors

A lower bound solution for the anchor problem is obtained by maximising the integral of the compressive stress along the soil anchor interface. As the individual normal stresses at element nodes on the soil/anchor boundary are allowed to differ, the anchor is implied to be rigid.

Finite element upper bound formulation

An upper bound on the exact pull-out capacity can be obtained by modelling a kinematically admissible velocity field. To be kinematically admissible, a velocity field must satisfy the set of constraints imposed by compatibility, the velocity boundary conditions and the flow rule. After prescribing a set of velocities along a specified boundary segment, we can equate the power dissipated internally (caused by plastic yielding within the soil mass and sliding of the velocity discontinuities) to the power dissipated by the external loads to yield a strict upper bound on the true limit load. An advantage of using the upper bound formulation of Sloan & Kleeman (1995) is that the direction of shearing along each velocity discontinuity is found automatically, and need not be specified a priori. A good indication of the likely failure mechanism can therefore be obtained without any assumptions being made in advance.

As in the lower bound case, a linear approximation to the Tresca yield surface is adopted to ensure that the formulation results in a linear programming problem. Unlike the lower bound formulation, however, this surface must be external to the parent yield surface to ensure that the solution found is a rigorous upper bound on the exact collapse load. This is achieved by adopting a p-sided prism that circumscribes the Tresca yield surface.

The three-noded triangle is again used for the upper bound formulation. Now, however, each node is associated with two unknown velocities, and each element has p non-negative plastic multiplier rates (where p is the number of sides in the linearised yield criterion). A linear variation of the velocities is assumed within each triangle. For each velocity discontinuity, there are also four non-negative discontinuity parameters that describe the velocity jumps along each triangle edge (see Sloan & Kleeman, 1995).

To define the objective function, the dissipated power (or some related load parameter) is expressed in terms of the unknown plastic multiplier rates and discontinuity parameters. As the soil deforms, power dissipation may occur in the velocity discontinuities as well as in the triangles.

Once the constraints and the objective function coefficients are assembled, a kinematically admissible velocity field is found that minimises the internal power dissipation for a specified set of boundary conditions.

A typical upper bound mesh for a horizontal anchor, along with the applied velocity boundary conditions, is shown in Fig. 4. A void is provided behind the anchor (line element) to ensure its immediate breakaway from the underlying soil. Modelling the anchor as a line element creates a series of velocity discontinuities between the face of the anchor and the soil, which can be assigned suitable material properties to simulate various interface conditions. For example, these velocity discontinuities are assigned a strength equal to the undrained shear strength of the soil for the case of a perfectly rough anchor, and a strength of zero for the case of a perfectly smooth anchor.

The finite element mesh arrangements (both upper and lower bound) were selected after considerable experimentation. This process involved adjustment of the mesh dimensions to ensure that the computed stress or velocity fields were contained, as well as providing a concentration of elements within critical regions. It is expected that any further mesh refinements would only lead to small variations in the estimated collapse load.

An upper bound solution is obtained by prescribing a unit velocity to the nodes along the line element that represents the anchor, subject to the constraint that it cannot move horizontally ($u = 0$) for horizontal anchors, or vertically ($v = 0$) for vertical anchors. After the corresponding optimization problem is solved for the imposed boundary conditions, the collapse load is found by equating the dissipated power to the power expended by the external forces.

RESULTS AND DISCUSSION

Finite element limit analyses were performed to obtain an upper and lower bound estimate of the anchor break-out factor, N_c, for the range of embedment depths and material properties previously mentioned. These results, along with the effects of plate roughness and overburden pressure, are discussed in the following sections. Where possible, past experimental and numerical results are compared with results obtained from the current study.

Analytical limit analysis and cavity expansion approach

By deriving several analytical solutions for the ultimate capacity of anchors, a useful check can be made on the bounds obtained from the numerical finite element scheme. As mentioned previously, both Rowe (1978) and Gunn (1980) were able to derive simple bound solutions for a horizontal anchor and trapdoor problem respectively. For comparison purposes the solutions of Gunn (1980) have been adopted for shallow horizontal anchors, while for deep horizontal anchors the solutions of Rowe have been used.

The upper bound theorem states that if a set of external loads can be found acting on a compatible failure mechanism such that the work done by these loads in an increment of displacement is equal to the work done by the internal stresses, these external loads are not lower than the true collapse load. In its simplest form the failure mechanism may be assumed to be composed of rigid blocks, and by examining different block arrangements the best (least) upper bound value can be found. The lower bound theorem states that if an equilibrium stress field covering the whole body can be found that balances a set of external loads on the stress boundary, and nowhere exceeds the material yield criterion, the external loads are not higher than the true collapse load. By examining different admissible stress states, the best (highest) lower bound value to the external loads can be found.

The three-variable block mechanism proposed by Gunn (1980) is shown in Fig. 5. By equating the power expended by the loads to the internal power dissipated along the discontinuities, and assuming failure occurs as a result of upward motion, this mechanism can be used to give an upper bound on the anchor break-out factor. After modifying this mechanism to include the variable ρ for inhomogeneous soils, the following expression for the anchor break-out factor is obtained:

$$
\begin{aligned}
N_{co} = \frac{q_u - \gamma H}{c_{uo}} = {} & \frac{\cos\beta[c_{uo} + \rho(H - z/2)]}{\cos\alpha \sin(\alpha + \beta)} \\
& + \frac{\sin(\alpha + \delta)[c_{uo} + \rho(H - y/2)]}{\sin(\beta - \delta)\sin(\alpha + \beta)} \\
& + \frac{\cos\beta\left[c_{uo} + \dfrac{\rho(y - z)}{z} + \rho(H - y)\right]}{\sin(\beta - \delta)\cos\delta} \\
& + 2\left(\frac{H}{B}\right)\frac{\cos\alpha \sin(\beta - \delta)\left[c_{uo} + \dfrac{\rho}{2}(H - y)\right]}{\sin(\alpha + \beta)\cos\delta} \\
& - \frac{\sin(\alpha + \delta)\sin\beta\left[c_{uo} + \dfrac{\rho}{2}(H - y)\right]}{\sin(\alpha + \beta)\cos\delta}
\end{aligned}
\tag{6}
$$

In the lower bound presented by Gunn, the exact plasticity solution for the expansion of a thick cylinder in homogeneous soil is used to construct a statically admissible stress field that leads to the following expression for the break-out factor:

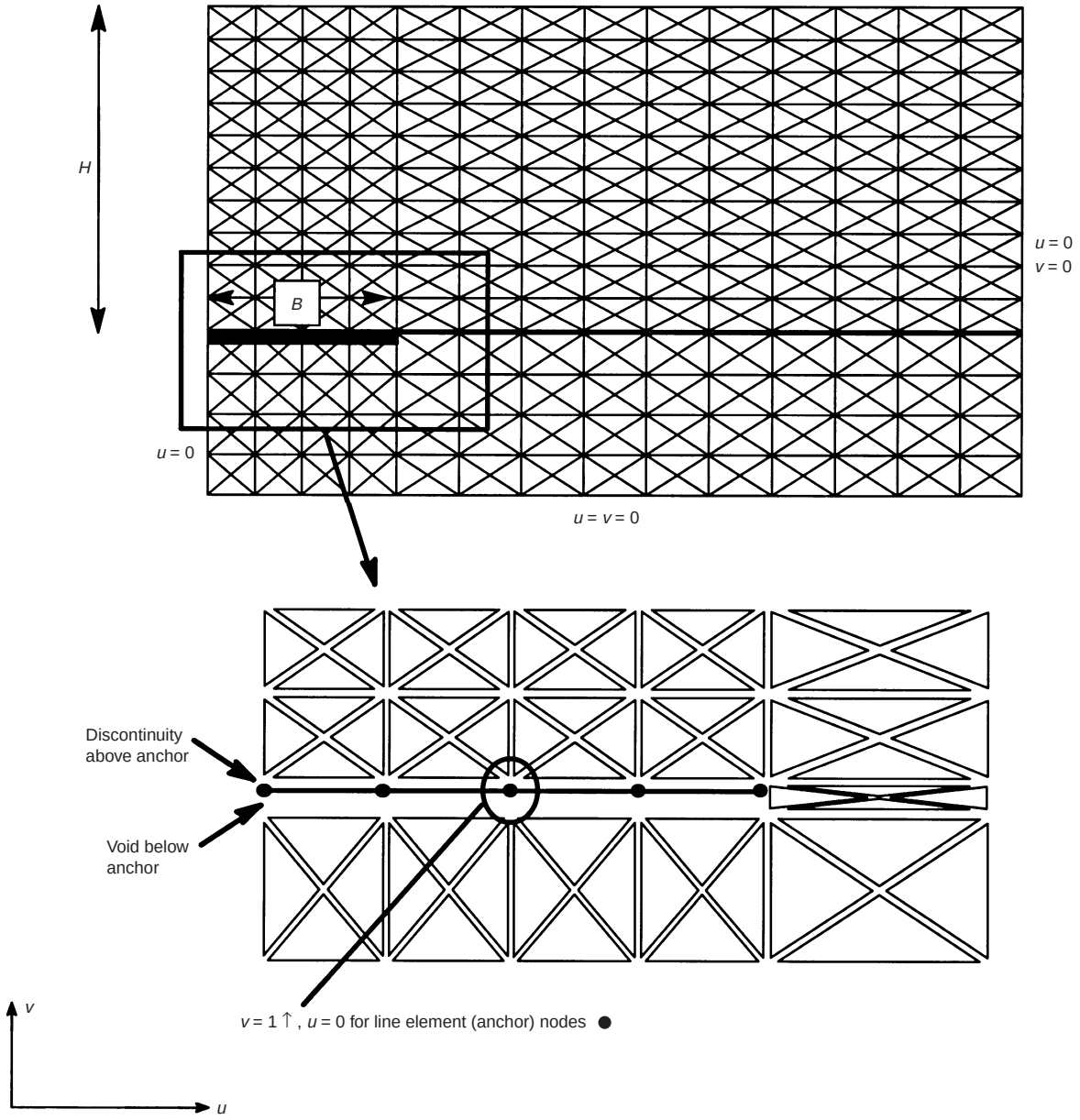

Fig. 4. Typical finite element upper bound mesh for horizontal anchors

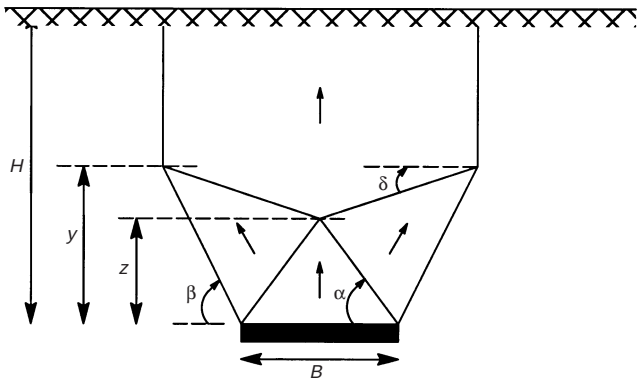

Fig. 5. Gunn upper bound mechanism

$$N_{co} = \frac{q_u - \gamma H}{c_u} = 2\log_e(2H/B), \qquad H/B \geqslant \frac{1}{2} \tag{7}$$

The above solutions of Gunn are shown in Fig. 6 for a range of embedment ratios. The discrepancy between the best upper and lower bounds is quite substantial, and increases with increasing H/B. By analysing more elaborate statically admissible stress fields and kinematically admissible velocity fields, better estimates of the break-out factor N_{co} could be found. This in turn would enable the true collapse load to be bracketed more closely. More elaborate mechanisms are, however, difficult to derive and prove admissible by analytical means.

As shown by Vesic (1971), it is also possible to use cavity expansion theory to predict the pull-out capacity of horizontal anchors in soils. Most recently, Yu (2000) has derived the following expression for the anchor break-out factor:

$$N_{co} = \frac{q_u - \gamma H}{c_u} = 2\log_e(2H/B) + 1 \tag{8}$$

This solution was based on the assumption that the break-out of a plate anchor will occur as soon as the plastic zone of soil (as calculated from cavity expansion theory) reaches the ground surface.

As shown in Fig. 2, the ultimate pull-out capacity does not continue to increase indefinitely with embedment depth, but reaches a maximum limiting value when the anchor failure mechanism becomes localised owing to the effect of overburden pressure. Although the critical embedment depth, H_{cr}, is a complex function of the overburden pressure and embedment

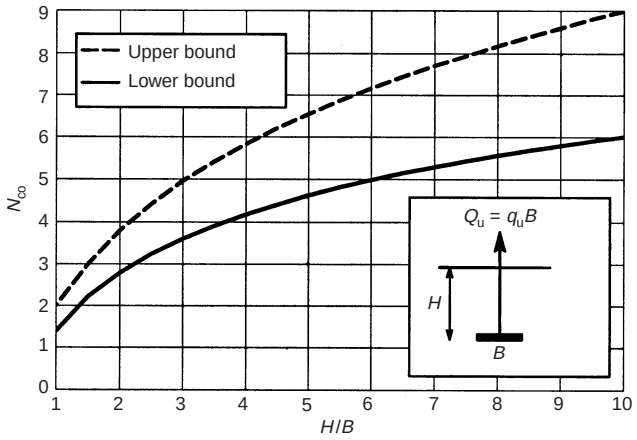

Fig. 6. Analytical bound solutions of Gunn: homogeneous soils

depth, the form of the deep failure mechanism essentially remains unaltered. Rowe (1978) postulated both a kinematically admissible upper bound solution and a statically admissible lower bound solution for a deep horizontal anchor (no breakaway) in homogeneous clay. These mechanisms are shown in Fig. 7, and are applicable to both rough and smooth anchors. For the case of a horizontal anchor, the stress field is antisymmetric about the anchor, and the lower bound and upper bound estimates of the break-out factor N_c^* are 10·28 and 11·42 respectively (the asterisk on N_c denotes deep failure). The finite element bound solutions obtained for a deep horizontal anchor will be compared with the analytical solutions of Rowe in a later section.

Any number of simple kinematically admissible mechanisms can be derived for a vertical anchor. Two such mechanisms are shown in Fig. 8. In these mechanisms an upper bound estimate of the break-out factor N_{co} can be obtained by equating the

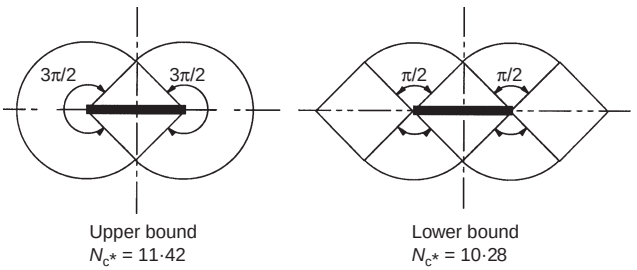

Fig. 7. Upper and lower bounds for deep horizontal anchors in homogeneous clay (no breakaway)

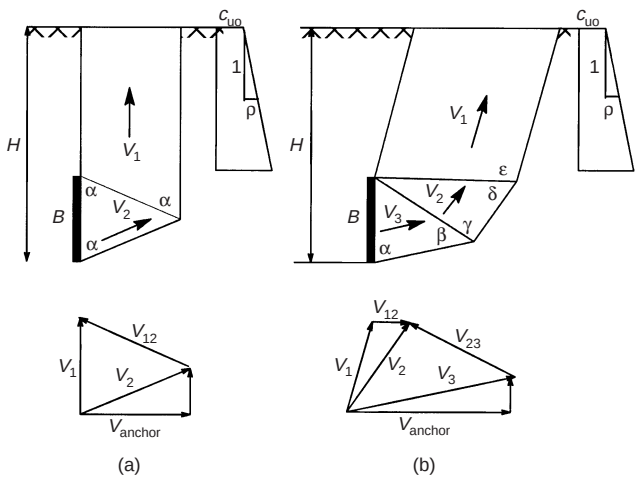

Fig. 8. Upper bound mechanisms for vertical anchors: (a) one-variable mechanism; (b) five-variable mechanism

external rate of work done by the anchor to the power dissipated by sliding along the discontinuities between adjacent blocks. Velocity diagrams are typically drawn as an aid to determining power dissipation along discontinuities. For the mechanisms shown in Fig. 8, the best (minimum) upper bound can be found by a numerical search for the critical values of the various angles. A comparison between the two mechanisms reveals that, for both homogeneous and inhomogeneous soil profiles, the best upper bounds are obtained from the five-variable mechanism over the range of H/B from 1 to 10.

The behaviour of deep vertical anchors in homogeneous soils will essentially be the same as for deep horizontal anchors (see Fig. 7).

Horizontal anchors in homogeneous soils

The computed upper and lower bound estimates of the anchor break-out factor N_{co} for homogeneous soils ($\rho = 0$) are shown graphically in Fig. 9. These results show that, for practical design purposes, sufficiently small error bounds were achieved, with the true value of the anchor break-out factor typically being bracketed to within ±5%. These error bounds are smaller for shallow embedment depths, being less than ±2·5% for ratios of H/B below 5.

The value of the break-out factor N_{co} obtained from the finite element limit analysis can be approximated by the following equations:

$$N_{co} = 2{\cdot}56 \log_e(2H/B) \qquad \text{Lower bound} \tag{9}$$

$$N_{co} = 2{\cdot}76 \log_e(2H/B) \qquad \text{Upper bound} \tag{10}$$

Figure 9(a) compares the finite element limit analysis solutions with the results of Gunn stated previously. It can be seen that the greatest improvement on the existing solutions of Gunn is provided by the lower bound technique. The analytical lower

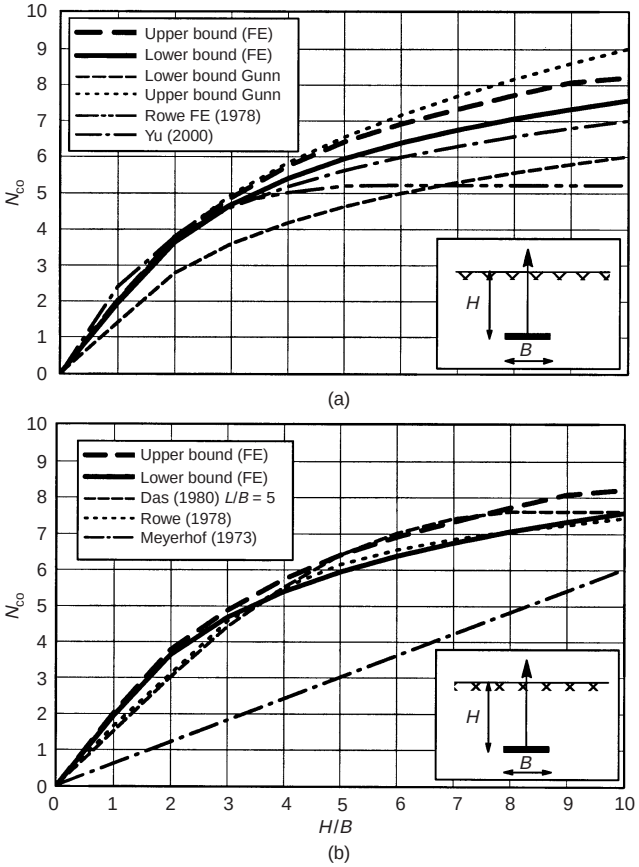

Fig. 9. Break-out factors for horizontal anchors in homogeneous soil: (a) comparison with existing numerical solutions; (b) comparison with existing laboratory test results

bound solution of Gunn is very conservative over the full range of embedment ratios, and is as much as 25% below the finite element lower bound solution. In contrast, while the finite element upper bounds improve on those of Gunn for anchors at larger embedment depths ($H/B > 4$), the Gunn mechanism is quite close to the optimal one for anchors where $H/B < 4$. This can be verified by comparing the failure mechanism predicted by Gunn with the finite element upper bound velocity field, as shown in Fig. 10(a). For a small embedment ratio ($H/B = 2$), the mechanism of Gunn is very similar to the finite element velocity field, while for greater embedment ratios ($H/B = 7$) the mechanism is no longer an accurate representation of the likely failure mode. The velocity fields shown in Fig. 10(a) are typical of the type of failure mode observed for horizontal anchors.

The cavity expansion solution of Yu (2000), given by equation (8), has also been plotted in Fig. 9(a). This solution compares favourably with the lower bound finite element predictions, and underestimates the break-out factor only slightly for ratios of $H/B > 3$.

The finite element solutions of Rowe & Davis (1982) have also been included in Fig. 9(a). For anchors at small embedment ratios ($H/B < 3$), these solutions plot very close to the upper and lower bound solutions, but appear to be grossly conservative for deeper embedment ratios. The reason for this latter discrepancy is the definition of failure adopted by Rowe & Davis. In their finite element analyses they found that, in many cases, the deformations prior to collapse were so great that for practical purposes failure could be deemed to have occurred at a load below the collapse load. For this type of problem, where

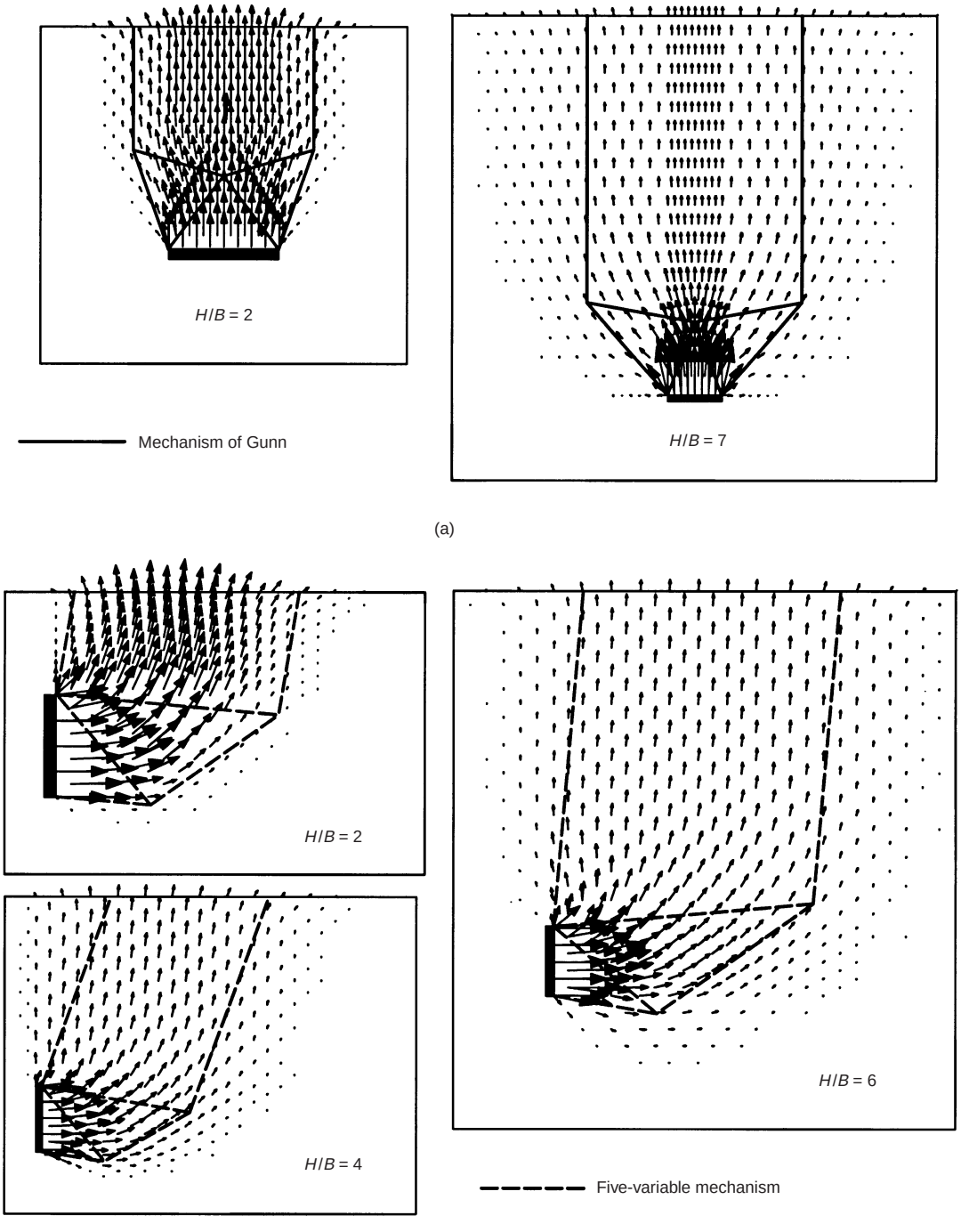

Fig. 10. Comparison of upper bound failure mechanisms for anchors in homogeneous clay ($\gamma H/c_u = 0$). Arrows indicate finite element upper bound velocity field

the ultimate capacity is reached only after large deformations, Rowe & Davis defined the failure load as the load that would give rise to a displacement four times that predicted by an elastic analysis. This was termed the k_4 failure criterion, and it is essentially a serviceability constraint on the ultimate load. For embedment ratios greater than 3 the collapse load was found to be limited by the k_4 condition, which explains the plateau of the curve shown in Fig. 9(a). This definition of failure is in contrast to that used in plasticity analysis, where failure is governed solely by the load-carrying capacity of the soil, and is reached when a significant portion of the soil mass has yielded and unrestrained plastic flow is imminent. By adopting the definition of failure suggested by Rowe & Davis, the ultimate capacity prediction will be obtained when the anchor is still in the range of contained plastic deformation prior to ultimate collapse.

A comparison of the finite element limit analysis results against a variety of laboratory model test results is shown in Fig. 9(b). These tests were performed using small model anchors, typically less than 50 mm wide. For such small anchors the depth of burial (H) need only be small. This reduces the physical size of the required model, and allows a large range of embedment ratios (H/B) to be analysed in the laboratory. Although convenient in terms of sample and model preparation, the overburden pressures are likely to be very small at these depths, and the term $\gamma H_a/c_u$ in equation (2) becomes insignificant. It is therefore reasonable to assume that, for comparison purposes, the break-out factor back-figured from laboratory tests is equivalent to N_{co} as given by equation (3). Based on this assumption, the test results of Das, Meyerhof and Rowe have been plotted in Fig. 9(b).

The test results of Rowe (1978) have been taken from the raw laboratory test data, and the curve shown in Fig. 9(b) represents a line of best fit. The results of Rowe compare favourably with the finite element limit analysis results and are close to the lower bound solution. The solutions of Das also compare well with the bound solutions, but are closer to the upper bound for embedment ratios (H/B) greater than about 4. Note that the tests of Rowe and Das were both performed on rectangular anchors with width-to-length ratios greater than or equal to 5. For comparison purposes it has been assumed that the anchor is essentially behaving as an infinite strip at these aspect ratios. Based on the observations of Rowe, who observed only small differences in pull-out capacity for anchors with aspect ratios of 5 and 8 respectively, this assumption appears to be reasonable.

The value of the break-out factor estimated using the approximate relationship suggested by Meyerhof (1973) is clearly over-conservative, and is as much as 50% below the finite element bound solutions.

Effect of overburden pressure. The numerical results discussed above have been limited to soil with no unit weight, and therefore the effect of soil weight (overburden) needs to be investigated. If our assumption of superposition is valid then it would be expected that the ultimate anchor capacity, as given in equations (1) and (2), would increase linearly with the dimensionless overburden pressure, $\gamma H_a/c_u$. The results from further lower bound analyses that include cohesion and soil weight, shown in Fig. 11, confirm that this is indeed the case. This conclusion is in agreement with the observations of Rowe (1978).

Figure 11 shows that the ultimate anchor capacity increases linearly with overburden pressure up to a limiting value. This limiting value reflects the transition from shallow to deep anchor behaviour where the mode of failure becomes fully contained around the anchor. At a given embedment depth, an anchor may behave as either shallow or deep, depending on the dimensionless overburden ratio, $\gamma H_a/c_u$. This is illustrated in Fig. 12, where an upper bound analysis has been performed on an anchor at an embedment ratio of 3. For this embedment ratio, the anchor behaves as a deep anchor once $\gamma H_a/c_u > 7$. The critical overburden ratio $\gamma H_a/c_u$, which marks the transition from shallow to deep anchor behaviour, reduces for increasing embedment ratios. For example, referring to Fig. 11, it is evident that the critical overburden ratio is approximately 3·5 for $H/B = 10$.

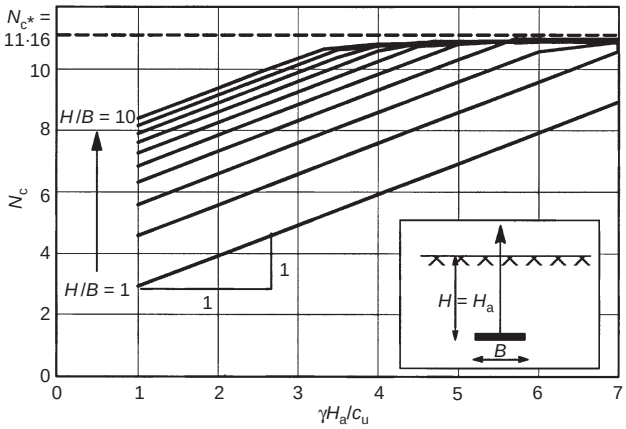

Fig. 11. Effect of overburden pressure (lower bound)

For deep anchors, the limiting values of the break-out factor N_{c*} were found to be 11·16 and 11·86. These values compare well with the analytical solutions of Rowe, who found lower and upper bounds of 10·28 and 11·42. The upper bound velocity field for a deep anchor, shown in Fig. 13, is similar to the analytical upper bound mechanism of Rowe (shown as a dashed line). For deep anchors, the form of the velocity field at collapse is essentially independent of the overburden pressure.

The velocity diagrams at collapse for shallow anchors, where the overburden pressure is insufficient to cause localised deep failure, are illustrated for various embedment ratios in Fig. 14. For anchors at small embedment ratios ($H/B = 1$) the failure mechanism consists of the upward movement of a rigid soil block immediately above the anchor. As the anchor embedment depth increases, the zone of plastic shearing extends outward from the anchor edges and causes an increase in the area over which deformations occur at the surface.

Effect of anchor roughness. The effect of anchor roughness on the break-out factor, N_{co}, was found to be almost linear with increasing embedment ratio (H/B). For an anchor with $H/B = 1$, for example, changing the roughness from perfectly rough to perfectly smooth reduces N_{co} by just 1%. For embedment ratios of $H/B = 5$, 8 and 10, this change in anchor roughness decreases N_{co} by 5%, 8% and 10% respectively. These results are consistent with the collapse velocity diagrams shown in Fig. 14. For embedment ratios greater than about 5, lateral shearing of the soil takes place at the anchor level and significant shear stresses are developed along a rough anchor/soil interface. In contrast, for $H/B = 1$, no velocity jump is observed along the anchor/soil interface as the rigid block of soil above the anchor moves vertically upwards.

Although a reduction in N_{co} of up to 10% was calculated for a smooth anchor, the ultimate anchor capacities are affected little by anchor roughness once the effects of overburden are included. A similar conclusion was reached by Rowe (1978). Unfortunately, the authors are not aware of any laboratory testing that has been performed to quantify the effects of anchor roughness.

Vertical anchors in homogeneous soils

The computed upper and lower bound estimates of the break-out factor N_{co} for a vertical anchor in homogeneous soil ($\rho = 0$) are shown graphically in Fig. 15. Small error bounds are again achieved, with the true value of the anchor break-out factor typically being bracketed to within ±3% over the range of embedment ratios.

The value of the break-out factor, N_{co}, determined from the finite element limit analyses can, with sufficient accuracy, be approximated by the following equation:

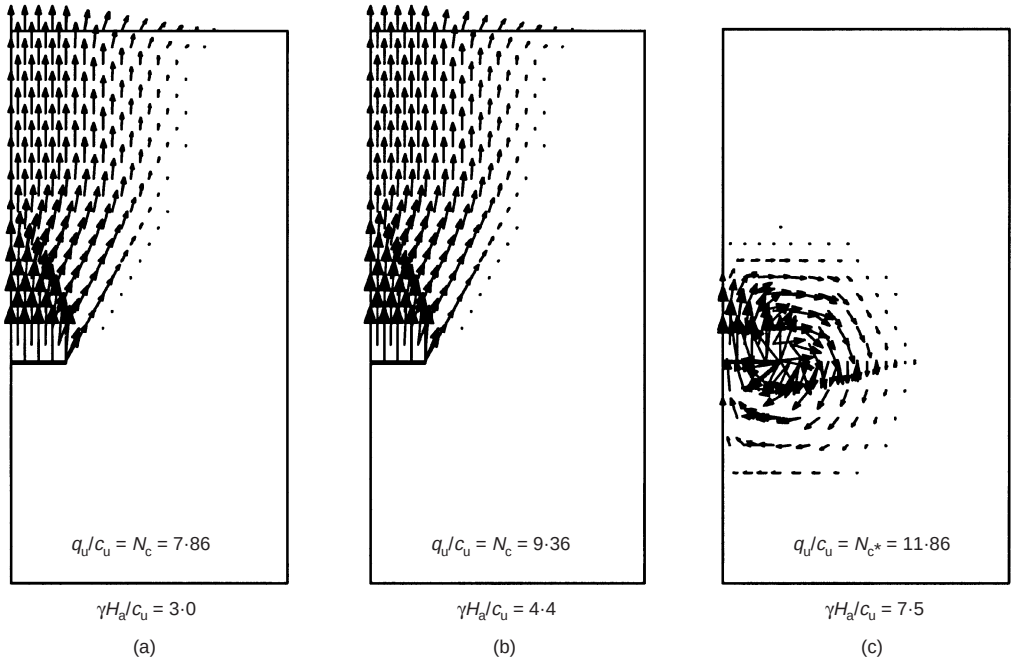

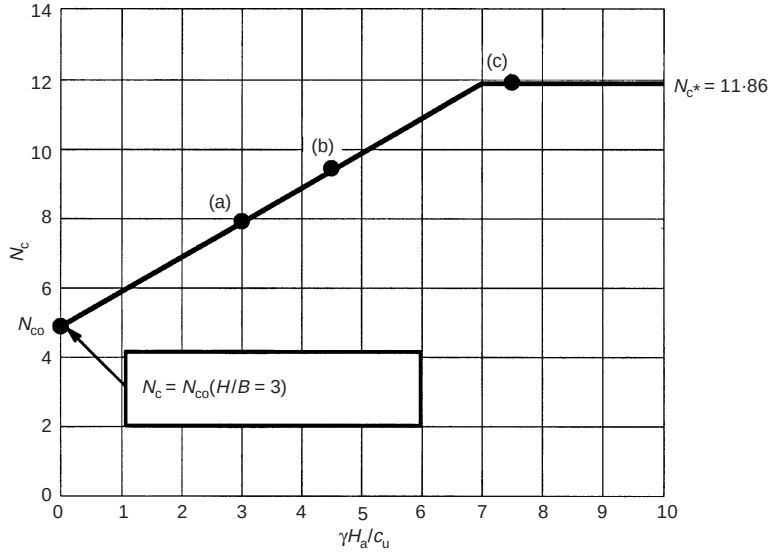

Fig. 12. Effect of overburden pressure, $H/B = 3$, homogeneous soil

$$N_{co} = 2{\cdot}46 \log_e(2H/B) + 0{\cdot}89 \quad \text{Lower bound} \quad (11)$$

$$N_{co} = 2{\cdot}58 \log_e(2H/B) + 0{\cdot}98 \quad \text{Upper bound} \quad (12)$$

The various numerical bound solutions and existing numerical and laboratory results for this case are compared in Figs 15(a) and 15(b) respectively.

Referring to Fig. 15(a), it is clear that the five-variable upper bound mechanism (Fig. 8(b)) is unable to model the true collapse mechanism accurately over the full range of embedment ratios. The reason for this is shown in Fig. 10(b), which compares the velocity fields for the various finite element upper bound analyses with the velocity fields predicted by the five-variable rigid block mechanism. Up to a ratio of $H/B = 3$, the rigid block and finite element collapse mechanisms are similar, and the computed solutions for N_{co} are typically within 3% of each other. For embedment ratios greater than 3, however, the rigid block mechanism is no longer a good representation of the true collapse mechanism, and the break-out factor N_{co} is overestimated by as much as 25%.

The results of Rowe (1978) are again difficult to compare against, owing to the k_4 definition of failure adopted. In the study by Rowe, the break-out factor was found to be limited by the k_4 definition of failure once H/B exceeds 2. Consequently, for embedment ratios above 2, the break-out factors determined by Rowe plot well below the finite element bound solutions.

Das *et al.* (1985a, 1985b) and Ranjan & Arora (1980) conducted a number of laboratory pull-out tests on vertical anchors with width to length ratios (L/B) varying from 1 (square) to 5 (rectangular). From the ultimate pull-out load obtained, the break-out factor N_c was back-calculated using an expression similar to equation (1). However, unlike equation (1), the ultimate pull-out load was assumed to be independent of the overburden pressure. This is clearly not the case at full scale, and therefore using these results, without adding the contribution due to unit weight, could lead to a very conservative estimate of the ultimate pull-out load. Owing to the use of small-scale model tests, the break-out factor determined by Das & Ranjan is again assumed equivalent to the break-out factor N_{co} given by equation (3). Fig. 15(b) shows the results of various pull-out tests on vertical anchors with an aspect ratio (L/B) of approximately 5. As for the horizontal anchor, it is assumed that at this aspect ratio the anchor is essentially

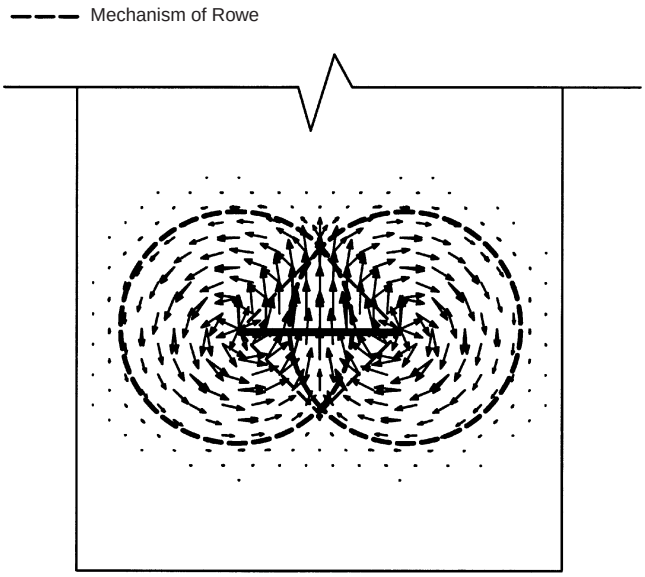

Fig. 13. Upper bound velocity field for a deep anchor

behaving as a strip. The results of Das & Ranjan compare reasonably well with the finite element bound solutions, tending to be slightly conservative for embedment ratios below 5.

The break-out factors determined by Meyerhof are again over-conservative, and plot as much as 35% below the finite element lower bound solutions.

Effect of overburden pressure. As was the case for horizontal anchors, the ultimate anchor capacity increases linearly with overburden pressure up to a limiting value that reflects the

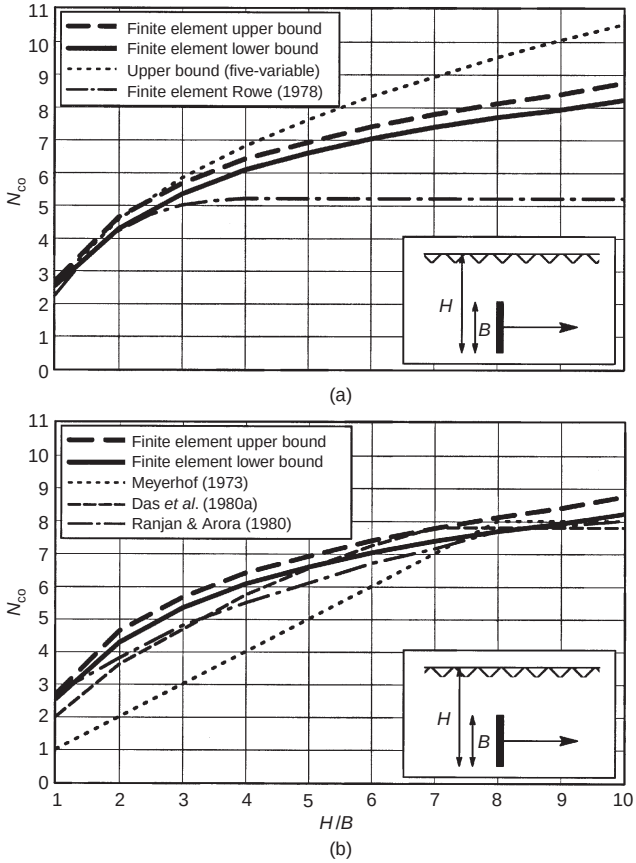

Fig. 15. Break-out factors for vertical anchors in homogeneous soil: (a) comparison with existing numerical solutions; (b) comparison with existing laboratory test results

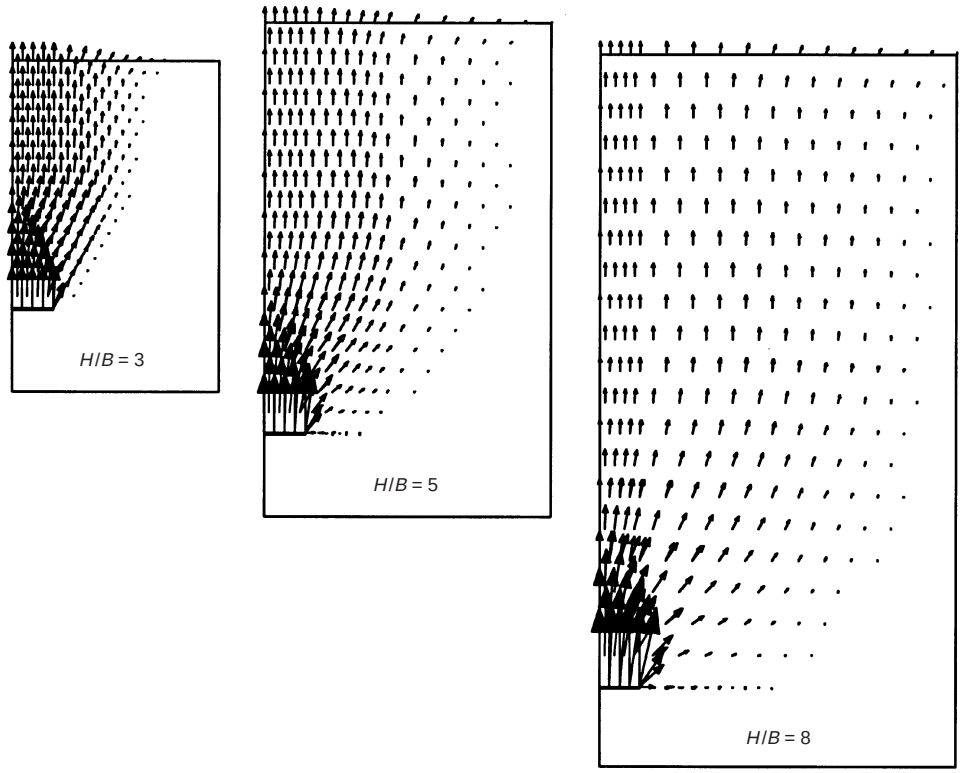

Fig. 14. Upper bound velocity fields for shallow anchors

transition from shallow to deep anchor behaviour. This is illustrated in Fig. 16, and confirms that the principle of superposition is valid.

For deep anchors, the limiting value of N_{c*} determined from the finite element lower and upper bound analyses was found to be 10·47 and 11·86 respectively. The upper bound value of 11·86 is identical to that determined for a horizontal anchor, while the lower bound result of 10·47 is approximately 6% below that determined for a deep horizontal anchor. Physically it would be expected that the limiting value of the break-out factor N_{c*} would be the same for both deep horizontal and deep vertical anchors. This follows from our assumption that the undrained shear strength is independent of the mean normal stress and thus the initial stress conditions.

For shallow anchors, the typical modes of failure are shown in the velocity diagrams of Fig. 10(b). As the anchor embedment ratio increases, the zone of plastic shearing increases to include an area of soil located above, behind and below the anchor.

Effect of anchor roughness. For embedment ratios (H/B) greater than or equal to 2, the anchor roughness is likely to have little influence on the ultimate anchor capacity. For these embedment ratios only small reductions ($<4\%$) in the break-out factor N_{co} were computed.

The ultimate capacity of a smooth vertical anchor with an embedment ratio less than 2 was found to be as much as 22% lower than that for a rough anchor. This agrees with the findings of Rowe & Davis (1982), where the reduction was found to be as high as 30%. The upper bound velocity diagram at collapse for anchors with an embedment ratio less than 2 shows that a large velocity jump exists at the soil/anchor interface: that is, the soil has moved (slipped) relative to the anchor. As discussed previously for the horizontal anchor, this indicates the development of significant shear stresses at the anchor/soil interface. These shear stresses are resisted by the interface and therefore contribute to the anchor's capacity.

Effect of increasing strength with depth

In reality, soil strength profiles are not homogeneous but may increase or decrease with depth or consist of distinct layers having significantly different properties. To ascertain the effect of a inhomogeneous soil on the capacity of an anchor, the specific case of a soil whose strength increases linearly with depth has been analysed. Although this is a common condition in the field, the authors are unaware of any attempts to determine its effect on anchor capacity.

For the case of a soil whose strength increases linearly with depth, the new break-out factor $N_{co\rho}$ is given by equation (5). Owing to the extra strength available, the magnitude of $N_{co\rho}$ will be greater than the break-out factor N_{co} (equation (3)) for a homogeneous soil with strength $c_u = c_{uo}$.

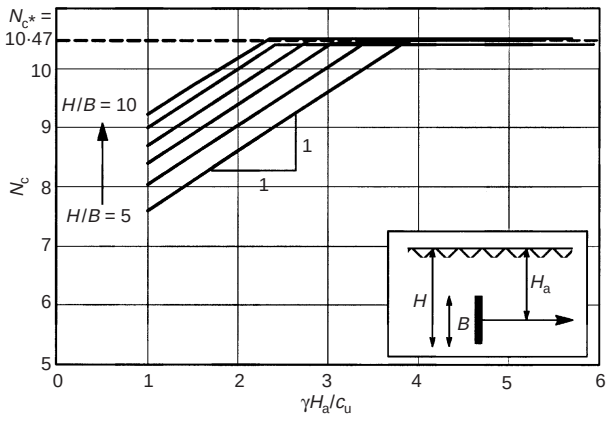

Fig. 16. Effect of overburden pressure (lower bound)

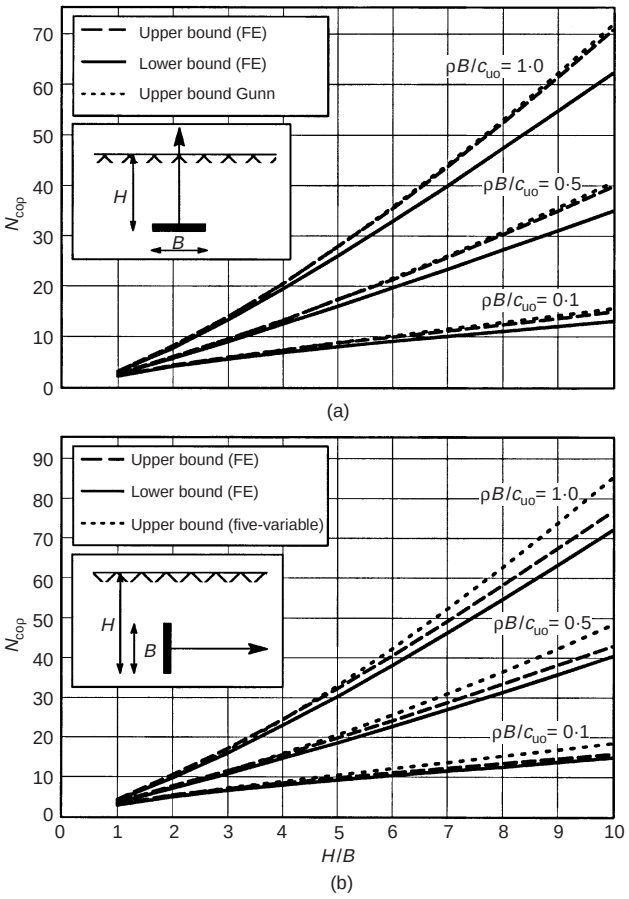

Fig. 17. Break-out factors for inhomogeneous soils

To cover most inhomogeneous problems of practical interest, the dimensionless ratio $\rho B/c_{uo}$ was varied between 0·1 and 1. For the sake of brevity, however, only the numerical results for cases of $\rho B/c_{uo} = 0{\cdot}1$, 0·5 and 1·0 are shown in Fig. 17. In reality, it is unlikely that the dimensionless ratio $\rho B/c_{uo}$ would be greater than about 0·2. Over the range of problems analysed, the error bounds on the true break-out factor are around $\pm 3\%$ for vertical anchors and vary from $\pm 3\%$ to $\pm 6\%$ for horizontal anchors.

Horizontal anchors. The break-out factors $N_{co\rho}$ determined for horizontal anchors, along with the rigid block solution of Gunn, are shown in Fig. 17(a). The Gunn mechanism gives solutions that are very close to the finite element upper bound solutions for all embedment ratios from 1 to 10. The reason for this good agreement is that the lateral extent of plastic yielding above the anchor is reduced by the assumed inhomogeneous soil profile. As a consequence, the mechanism of Gunn predicts the true failure mechanism better than it does for a homogeneous soil.

By using Fig. 17(a), an expression for the pullout factor $N_{co\rho}$ can be derived as a function of the embedment ratio H/B. However, this requires a separate equation for each strength profile $\rho B/c_{uo}$. Clearly, for design purposes, a single parametric equation that can be used for a whole range of strength profiles is more desirable.

In deriving such a parametric equation it is expected that the pullout factor $N_{co\rho}$ will be a function of the dimensionless variables $\rho B/c_{uo}$ and H/B (or $\rho H/c_{uo}$). Referring to Fig. 18(a), it appears that a unique relation exists between the ratio $N_{co\rho}/N_{co}$ and the dimensionless ratio $\rho B(2H/B - 1)/2c_{uo}$. Both the lower bound and upper bound results (approx. 220 data points) are presented on this figure and in most cases are within 1–2% of each other. By inserting a line of best fit through the data, the break-out factor can approximated by

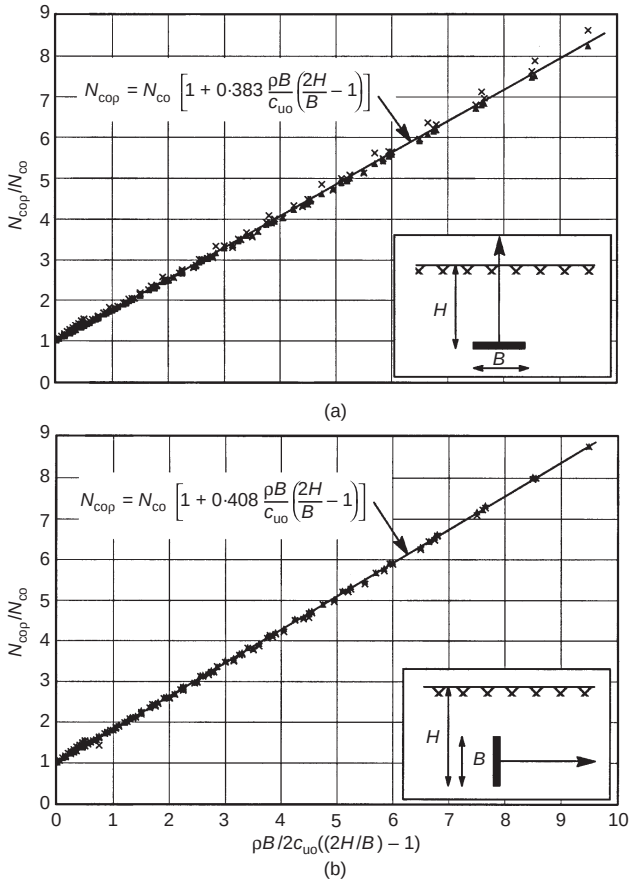

Fig. 18. Effect of increasing soil cohesion: lower bound results

$$N_{co\rho} = N_{co}\left[1 + 0{\cdot}383\frac{\rho B}{c_{uo}}\left(\frac{2H}{B} - 1\right)\right] \tag{13}$$

where, for a safe design, N_{co} is given by equation (9).

This equation can be confirmed by reproducing the plot in Fig. 18(a) using the rigid block results obtained using the mechanism of Gunn.

The effect of unit weight has also been investigated, and it was again found that the ultimate anchor capacity increases linearly with overburden pressure up to a limiting value. At this point there is a transition from shallow to deep anchor behaviour. Based on the finite element bound results, the limiting value of the break-out factor $N_{c\rho^*}$ can be approximated by

$$N_{c\rho^*} = N_{c^*}\left(1 + \frac{\rho H}{c_{uo}}\right) \tag{14}$$

where $N_{c^*} = 11{\cdot}16$. The form of equation (14) suggests that the ultimate capacity of deep horizontal anchors in the assumed inhomogeneous soil profile is simply a function of the soil cohesion at the anchor level. From equation (4), $N_c = N_{c\rho^*}$, and substituting equation (14) into equation (1) yields

$$q_u = c_{uo}N_{c^*}\left(1 + \frac{\rho H}{c_{uo}}\right)$$
$$= N_{c^*}c_u(H)$$

where $c_u(H)$ = the soil cohesion at depth H below the ground level.

The observed upper bound velocity diagram for deep horizontal anchors is essentially the same as that shown in Fig. 13, irrespective of the rate of strength increase, ρ.

Vertical anchors. The break-out factors $N_{co\rho}$ determined from the finite element formulations, along with the five-variable rigid block solutions derived previously, are shown in Fig. 17(b). The rigid block predictions are close to the finite element upper bounds for $H/B < 5$ but, for ratios greater than this, tend to overestimate the break-out factor by up to 15%. This represents a small improvement compared with the results obtained for homogeneous soils where, for larger embedment ratios, the overprediction was around 25%.

For design purposes, a single parametric equation for the breakout factor $N_{co\rho}$ can again be obtained by quantifying the trend shown in Fig. 18(b). By inserting a line of best fit through the data, the break-out factor can be approximated by

$$N_{co\rho} = N_{co}\left[1 + 0{\cdot}408\frac{\rho B}{c_{uo}}\left(\frac{2H}{B} - 1\right)\right] \tag{15}$$

The inclusion of overburden pressure again produces a linear increase in the ultimate anchor capacity up to a limiting value. The limiting value of the break-out factor $N_{c\rho^*}$ can be approximated by

$$N_{c\rho^*} = N_{c^*}\left[1 + \frac{\rho B}{2c_{uo}}\left(\frac{2H}{B} - 1\right)\right] \tag{16}$$

By substituting equation (16) into equation (1), we see that the ultimate capacity of a deep vertical anchor in inhomogeneous soil is a function of the soil cohesion at anchor level. This implies that $q_u = N_{c^*}c_u(H_a)$, where $N_{c^*} = 10{\cdot}47$.

SUGGESTED PROCEDURE FOR ESTIMATION OF UPLIFT CAPACITY

1. Determine representative values of the material parameters c_{uo}, ρ and γ.
2. Knowing the anchor size B and embedment depth H, calculate the embedment ratio H/B and overburden ratio $\gamma H_a/c_{uo}$.
3. Calculate the break-out factor N_{co} using equation (9) or (11) depending on the anchor orientation.
4. Adopt $N_{c^*} = 11{\cdot}16$ for horizontal anchors, and $N_{c^*} = 10{\cdot}47$ for vertical anchors.
5. For homogeneous soils:
   (i) Calculate the break-out factor N_c using equation (2).
   (ii) If $N_c \geqslant N_{c^*}$ then the anchor is a deep anchor. The ultimate pull-out capacity is given by equation (1), where $N_c = N_{c^*} = 11{\cdot}16$.
   (iii) If $N_c \leqslant N_{c^*}$ then the anchor is a shallow anchor. The ultimate pull-out capacity is given by equation (1), where N_c is the value obtained in 5(i).
6. For inhomogeneous soils:
   (i) Calculate the break-out factor $N_{co\rho}$ using equation (13) or (15). The value of N_{co} is that found in 3.
   (ii) Calculate the breakout factor N_c using equation (4).
   (iii) Calculate the limiting value of the break-out factor $N_{c\rho^*}$ using equation (14) or (16). The value of N_{co} is that found in 3.
   (iv) If $N_c \geqslant N_{c\rho^*}$ then the anchor is a deep anchor. The ultimate pull-out capacity is given by equation (1), where $N_c = N_{c\rho^*}$.
   (v) If $N_c \leqslant N_{c\rho^*}$ then the anchor is a shallow anchor. The ultimate pull-out capacity is given by equation (1), where N_c is the value obtained in 6(ii).

CONCLUSIONS

Rigourous lower and upper bound solutions for the ultimate capacity of horizontal and vertical strip anchors in both homogeneous and inhomogeneous clay soils have been presented. Consideration has been given to the effect of anchor embedment depth, anchor roughness, material homogeneity and overburden pressure. Results are for the case where no suction forces exist between the anchor and soil, which constitutes what is known as the 'immediate breakaway' condition.

The results obtained have been presented in terms of familiar

break-out factors in both graphical and numerical form to facilitate their use in solving practical design problems. A systematic design approach has also been proposed.

The following conclusions can be drawn from the results presented in this paper:

(*a*) For most cases in this study, it is found that the exact anchor capacity can be predicted to within ±5% using numerical finite element formulations of the lower and upper bound limit theorems.
(*b*) Existing numerical solutions can differ from the bound solutions by up to ±25% for a homogeneous soil, with a slight reduction in error for an inhomogeneous soil whose strength increases linearly with depth. The exising solutions are typically in greatest error when the embedment ratio is relatively large ($H/B > 4$).
(*c*) The bound solutions compare well with published results from small-scale laboratory tests.
(*d*) The ultimate capacity for all anchors was found to increase linearly with overburden pressure up to a limiting value. This limiting value reflects the transition from shallow to deep anchor behaviour where the mode of failure becomes localised around the anchor. At a given embedment depth, an anchor may behave as shallow or deep, depending on the dimensionless overburden ratio $\gamma H_a/c_u$. For cases that do not fail in a deep mode, the principle of superposition is valid.
(*e*) Anchor roughness was found to increase the ultimate capacity of vertical anchors with embedment ratios less than 2 by as much as 22%. The ultimate capacity of horizontal anchors is less affected by anchor roughness.
(*f*) A relationship between the capacity of anchors in homogeneous and inhomogeneous soil profiles has enabled simple parametric equations to be produced. These equations can be used to solve practical design problems.

REFERENCES

Ashbee, R. A. (1969). *A uniaxial analysis for use in uplift foundation calculations*, Report RD/L/R 1608. Central Electricity Research Laboratory.

Das, B. M. (1978). Model tests for uplift capacity of foundations in clay. *Soils Found.* **18**, No. 2, 17–24.

Das, B. M. (1980). A procedure for estimation of ultimate capacity of foundations in clay. *Soils Found.* **20**, No. 1, 77–82.

Das, B. M. (1990). *Earth anchors*. Amsterdam: Elsevier.

Das, B. M., Tarquin, A. J. & Moreno, R. (1985a). Model tests for pullout resistance of vertical anchors in clay. *Civil Engng for Practising and Design Engineers*, **4**, No. 2, 191–209.

Das, B. M., Moreno, R. & Dallo, K. F. (1985b). Ultimate pullout capacity of shallow vertical anchors in clay. *Soils Found.* **25**, No. 2, 148–152.

Davie, J. R. & Sutherland, H. B. (1977). Uplift resistance of cohesive soils. *J. Soil Mech. Found. Div. ASCE* **103**, No. 9, 935–952.

Gunn, M. J. (1980). Limit analysis of undrained stability problems using a very small computer. *Proceedings of the symposium on computer applications in geotechnical problems in highway engineering*, Cambridge University, pp. 5–30.

Merifield, R. S., Sloan, S. W. & Yu, H. S. (1997). *Rigorous plasticiy solutions for the bearing capacity of two-layered clays*, Research Report 157.11.1997. Department of Civil, Surveying and Environmental Engineering, University of Newcastle. *Geotechnique* **49**, No. 4, 471–490.

Meyerhof, G. G. (1973). Uplift resistance of inclined anchors and piles. *Proc. 8th Int. Conf. Soil Mech. Found. Engng, Moscow* **2.1**, 167–172.

Meyerhof, G. G. & Adams, J. I. (1968). The ultimate uplift capacity of foundations. *Can. Geotech. J.* **5**, No. 4, 225–214.

Ranjan, G. & Arora, V. B. (1980). Model studies on anchors under horizontal pull in clay. *Proc. 3rd Aust. N. Z Conf. Geomech., Wellington* **1**, 65–70.

Rowe, R. K. (1978). *Soil structure interaction analysis and its application to the prediction of anchor behaviour.* PhD thesis, University of Sydney, Australia.

Rowe, R. K. & Davis, E. H. (1982). The behaviour of anchor plates in clay. *Géotechnqiue* **32**, No. 1, 9–23.

Sloan, S. W. (1988). Lower bound limit analysis using finite elements and linear programming. *Int. J. Numer. Anal. Methods Geomech.* **12**, 61–67.

Sloan, S. W. & Kleeman, P. W. (1995). Upper bound limit analysis using discontinuous velocity fields. *Comput. Methods Appl. Mech. Engng* **127**, 293–314.

Sloan, S. W. & Assadi, A. (1991). Undrained stability of a square tunnel in a soil whose strength increases linearly with depth. *Computers and Geotechnics*, **12**, 321–346.

Sloan, S. W. & Assadi, A. (1992). The stability of tunnels in soft ground. Proceedings of Peter Wroth Memorial Symposium on Predictive Soil Mechanics, Oxford, 644–663.

Sloan, S. W., Assadi, A. & Purushothaman, N. (1990). Undrained stability of a trapdoor. *Géotechnique* **40**, 45–62.

Ukritchon, B., Whittle, A. J. & Sloan, S. W. (1998). Undrained limit analysis for combined loading of strip footings on clay. *J. Geotech. Geoenvironmental Engng, ASCE* **124**, No. 3, 265–276.

Vesic, A. S. (1971). Breakout resistance of objects embedded in ocean bottom. *J. Soil Mech. Found. Div. ASCE* **97** No. 9, 1183–1205.

Yu, H. S. (2000). *Cavity expansion methods in geomechanics*. Dordrecht: Kluwer.

Yu, H. S. & Sloan, S. W. (1994). A note on bearing capacity of soft clays under embankments. *J. Geotech. Geoenvironmental Engng, ASCE* **120**, No. 1, 246–255.

Yu, H. S. & Sloan, S. W. (1997). Finite element limit analysis of reinforced soils. *Comput. Struct.* **63**, No. 3, 567–577.

Yu, H. S., Salgado, R., Sloan, S. W. & Kim, J. M. (1998). Limit analysis versus limit equilibrium for slope stability. *J. Geotech. Geoenvironmental Engng, ASCE* **124**, No. 1, 1–11.